AJNR

FLAIR^2: A Combination of FLAIR and T2 for Improved MS Lesion Detection

V. Wiggermann, E. Hernández-Torres, A. Traboulsee, D.K.B. Li and A. Rauscher

AJNR Am J Neuroradiol 2016, 37 (2) 259-265
doi: https://doi.org/10.3174/ajnr.A4514
http://www.ajnr.org/content/37/2/259

FLAIR^2: A Combination of FLAIR and T2 for Improved MS Lesion Detection

V. Wiggermann, E. Hernández-Torres, A. Traboulsee, D.K.B. Li, and A. Rauscher

ABSTRACT

BACKGROUND AND PURPOSE: FLAIR and double inversion recovery are important MR imaging scans for MS. The suppression of signal from CSF in FLAIR and the additional suppression of WM signal in double inversion recovery improve contrast between lesions, WM and GM, albeit at a reduced SNR. However, whether the acquisition of double inversion recovery is necessary is still debated. Here, we present an approach that allows obtaining CSF-suppressed images with improved contrast between lesions, WM and GM without strongly penalizing SNR.

MATERIALS AND METHODS: 3D T2-weighted and 3D-FLAIR data acquired from September 2014 to April 2015 in healthy volunteers (23.4 ± 2.4 years of age; female/male ratio, 3:2) and patients (44.1 ± 14.0 years of age; female/male ratio, 4:5) with MS were coregistered and multiplied (FLAIR^2). SNR and contrast-to-noise measurements were performed for focal lesions and GM and WM. Furthermore, data from 24 subjects with relapsing-remitting and progressive MS were analyzed retrospectively (52.7 ± 8.1 years of age; female/male ratio, 14:10).

RESULTS: The GM-WM contrast-to-noise ratio was by 133% higher in FLAIR^2 than in FLAIR and improved between lesions and WM by 31%, 93%, and 158% compared with T2, DIR, and FLAIR, respectively. Cortical and juxtacortical lesions were more conspicuous in FLAIR^2. Furthermore, the 3D nature of FLAIR^2 allowed reliable visualization of callosal and infratentorial lesions.

CONCLUSIONS: We present a simple approach for obtaining CSF suppression with an improved contrast-to-noise ratio compared with conventional FLAIR and double inversion recovery without the acquisition of additional data. FLAIR^2 can be computed retrospectively if T2 and FLAIR scans are available.

ABBREVIATIONS: CNR = contrast-to-noise ratio; DIR = double inversion recovery

MR imaging is important for the diagnosis and monitoring of MS. Formation of MS lesions creates a hydrophilic environment, resulting in an increase in the T2 and proton density–weighted MR signal and a signal reduction on T1-weighted scans.[1] Ovoid hyperintense areas on T2-weighted MR imaging are therefore a radiologic hallmark of MS. Lesion conspicuity is often affected by the bright CSF signal, for instance, close to the ventricles or cortical sulci. FLAIR is a T2-weighted scan that suppresses CSF selectively with an inversion pulse.[2] Yet, the CSF signal suppression comes at the cost of reduced SNR. Usually, FLAIR scans are acquired in 2D with sections parallel to the subcallosal line. Additional sagittal FLAIR scans are required to reliably detect corpus callosum lesions.[2,3] Furthermore, 2D-FLAIR has artifacts due to CSF and blood inflow and often provides insufficient T2-weighting,[4] requiring additional proton density/T2-weighted images for the detection of lesions in infratentorial areas. The brain MR imaging protocol for MS studies[5] includes proton density and T2-weighted spin-echo, axial, and sagittal FLAIR and recommends pre- and postcontrast T1-weighted spin-echo MR imaging.

Apart from diagnosis, conventional MR images play an im-

Received May 4, 2015; accepted after revision June 21.

From the Departments of Physics and Astronomy (V.W.), Pediatrics (V.W., E.H.T., A.R.), Medicine (Neurology) (A.T., D.K.B.L.), and Radiology (D.K.B.L.); and University of British Columbia MRI Research Centre (V.W., E.H.T., A.R.); Centre for Brain Health (D.K.B.L., A.R.); and Child and Family Research Institute (A.R.), University of British Columbia, Vancouver, British Columbia, Canada.

This work was supported by a graduate studentship award from the MS Society of Canada (EGID 2002 [V.W.]), a Canadian Institutes of Health Research New Investigator Award (261306 [A.R.]), and a postdoctoral award by Consejo Nacional de Ciencia y Tecnologia (237961 [E.H.T.]).

Paper previously presented at: 23rd Annual Meeting of the International Society for Magnetic Resonance in Imaging, May 30–June 5, 2015; Toronto, Ontario, Canada.

Please address correspondence to Alexander Rauscher, PhD, UBC MRI Research Centre and Department of Pediatrics, G33 Purdy Pavilion, 2221 Wesbrook Mall, University of British Columbia, Vancouver, BC, V6T 2B5, Canada; e-mail: rauscher@physics.ubc.ca; @rauscherMRI

Indicates open access to non-subscribers at www.ajnr.org
Indicates article with supplemental on-line photos.
http://dx.doi.org/10.3174/ajnr.A4514

Table 1: Imaging parameter overview for the SNR/CNR estimations and the retrospectively analyzed patient study

Study	Sequence	$TR/TE_{eff}/TE_{equiv}/TI_1/TI_2$ (ms)	Acq. Voxel Size (mm^3)	Recon. Voxel Size (mm^3)	SENSE Acceleration	Acquisition Time (min)
SNR	FLAIR	8000/353/162/2400	0.8 × 0.8 × 1.6	0.8 × 0.8 × 0.8	2.5 (AP)2 (RL)	6:16
SNR	T2	2500/363/133	1 × 1 × 1.6	0.8 × 0.8 × 0.8	2 (AP) 2 (RL)	3:33
SNR	DIR	8000/337/156/3200/500	1 × 1 × 2	1 × 1 × 1	2.5 (AP) 2 (RL)	7:52
RS	FLAIR	8000/337/156/2400	1 × 1 × 1.6	0.8 × 0.8 × 0.8	2.5 (AP) 2 (RL)	5:04
RS	T2	2500/363/133	1 × 1 × 1.6	0.8 × 0.8 × 0.8	2 (AP) 1.5 (RL)	4:42
RS	DIR	8000/337/156/3200/500	1 × 1 × 1.6	0.8 × 0.8 × 0.8	2.5 (AP) 2 (RL)	9:44

Note:—RS indicates retrospectively analyzed patient study; Acq., acquired; Recon., reconstructed; SENSE, sensitivity encoding; AP, anterior-posterior; RL, right-left; TE_{equiv}, TE equivalent; TE_{eff}, effective TE.

portant role as outcome measures in clinical trials of new MS therapies.[5,6] New lesion activity (eg, gadolinium-enhancing lesions and new or enlarging T2-lesions) and estimates of disease burden (eg, total T2-lesion volume or count; T1-hypointense lesion volume; brain atrophy) are typical imaging end points in clinical trials.[5] These scans are directed toward lesion identification in WM. Demyelination and the appearance of lesions is, however, not limited to the WM; it also involves the deep and cortical GM.[7] Focal GM lesions appear in the earliest stages of MS[8,9] and are associated with physical and cognitive disability.[10,11] Moreover, cortical lesion load was shown to be a predictor of progression of clinical disability during 5 years[12] and to improve predictions for the conversion from relapsing-remitting to secondary-progressive MS compared with assessing WM lesions alone.[13] Given the importance of cortical lesions in MS, there is great interest in their visualization. However, the cortex is thin, its myelin content is low, and inflammation is low in cortical lesions. Contrast between lesions and healthy tissue is therefore low, making the detection of cortical damage challenging.

In double inversion recovery (DIR),[14] both CSF and the WM signal are suppressed; this suppression results in enhanced contrast between lesions, GM and WM. T1-relaxation times of GM and WM are similar. Therefore, both tissues are affected by the inversion pulse, resulting in reduced SNR. Long data-acquisition times further limit the spatial resolution of DIR to 1 mm^3 isotropic at 3T. In a postmortem study, the specificity of 3D-DIR was found to be 90%, whereas sensitivity was only 18%.[15] DIR detected most leukocortical lesions; however, intracortical and subpial lesions were still missed.[15] Intracortical and subpial lesions are the most common cortical lesions in patients with chronic MS, yet subpial lesions are rarely detected with DIR or other techniques.[16,17] More recently, 3D versions of MR imaging sequences for MS have become available[18] but are not yet used widely in clinical imaging of MS.[19] 3D sequences with isotropic voxels of 1 mm^3 volume or smaller are particularly suitable for the assessment of the cortex. Moreover, these scans allow simultaneous assessment of all 3 orthogonal image planes. A drawback is the increased acquisition time per scan, in particular for DIR. Lesion detection, especially within the cortex, would benefit from a rapid 3D imaging approach with high spatial resolution, suppressed CSF, higher SNR than DIR, and a good contrast-to-noise ratio (CNR) between lesions, GM and WM.

This study aims to develop and test a method that combines the good SNR of T2-weighted images with the CSF suppression of FLAIR to achieve GM-WM contrast similar to that in DIR and good contrast between lesions, healthy tissue. We compared SNR and CNR of this new approach with conventional FLAIR, T2, and DIR; and we present images acquired in patients with relapsing-remitting and progressive MS.

MATERIALS AND METHODS

The Clinical Research Ethics Board of University of British Columbia approved the protocol. All subjects gave written informed consent in accord with the Declaration of Helsinki. The authors declare that there is no conflict of interest.

Subjects

Five healthy volunteers (23.4 ± 2.4 years of age; female/male ratio, 3:2) and 9 subjects with MS (44.1 ± 14.0 years of age; female/male ratio, 4:5, median Expanded Disability Status Scale score, 2.5; and mean disease duration, 10.4 ± 6.7 years; 6 with relapsing-remitting, 2 with primary-progressive MS, 1 with secondary-progressive MS) underwent MR imaging for this study. Furthermore, data from 24 subjects with MS (17 relapsing-remitting, 4 secondary-progressive MS, 3 primary-progressive MS; mean age, 52.7 ± 8.1 years; female/male ratio, 14:10; median Expanded Disability Status Scale score, 3.5; and mean age of disease onset, 38.2 ± 10.2 years) were analyzed retrospectively.

MR Imaging Protocol

MR imaging data were acquired on a 3T scanner (Achieva; Philips Healthcare, Best, the Netherlands) equipped with an 8-channel sensitivity encoding head coil. The imaging protocol included sagittal 3D-T2, 3D-FLAIR, and 3D-DIR scans. Detailed imaging parameters used for the CNR/SNR measurements and the retrospectively analyzed patient study are listed in Table 1.

The MR imaging protocol was refined after the study in the 24 patients and in parallel with the measurements of SNR and CNR. A range of spatial resolutions was tested in patients and controls. The specific imaging parameters are listed in the respective figure captions.

Data Processing and SNR/CNR Estimates

3D-FLAIR images were registered into the 3D T2 space by using FLIRT (FMRIB Linear Image Registration Tool; http://www.fmrib.ox.ac.uk)[20,21] (12 *df*, search angle of 10°, mutual information as a cost function, sinc interpolation) and then multiplied with the T2 image, resulting in a heavily T2-weighted, CSF-suppressed image, which we refer to as $FLAIR^2$ (FLAIR squared).

For SNR and CNR measurements, every scan was acquired twice. The 2 consecutively acquired T2-weighted images were used to create a T2 half-way space by image registration with FLIRT.[20,21] FLAIR and DIR images were then registered into the half-way space by using FLIRT with 6 *df*, a search angle of 10°, and

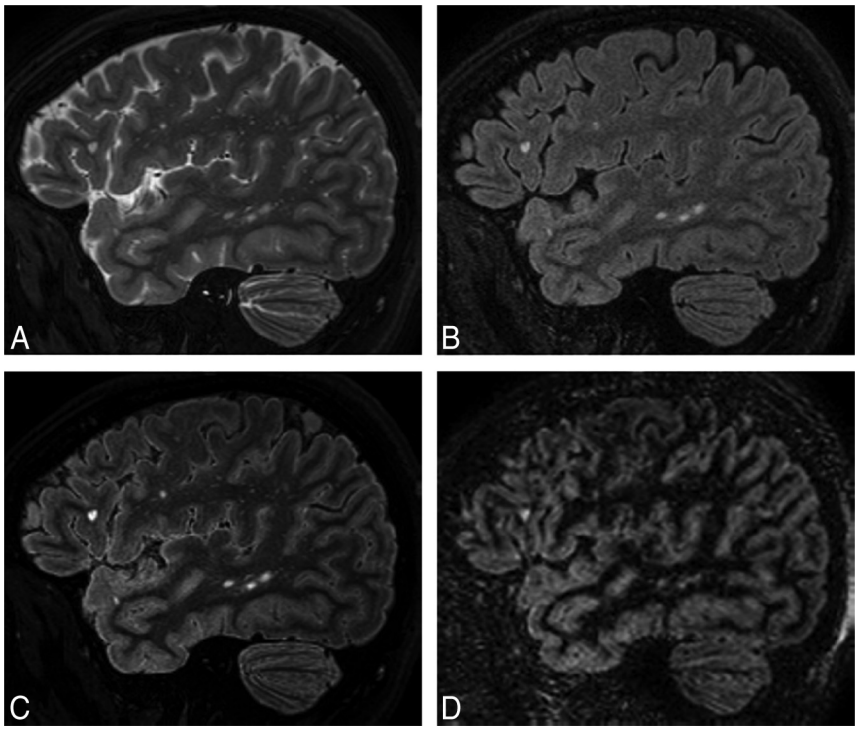

FIG 1. Comparison of standard MR images of MS with FLAIR^2 within the same patient (a 35-year-old woman): T2 (*A*), FLAIR (*B*), FLAIR^2 (*C*), and DIR (*D*). Here, T2 and FLAIR were acquired at 0.67 × 0.76 × 1.34 mm^3 within 6 minutes and 8 seconds and 7 minutes and 51 seconds, respectively, and were reconstructed to isotropic 0.3-mm^3 voxels, resulting in exquisite image contrast of the FLAIR^2 image compared with DIR (acquired within 13 minutes and 35 seconds and reconstructed to 1 mm^3), however, with much higher SNR. FLAIR^2 exhibits the highest contrast-to-noise levels between GM and WM and between lesions and surrounding normal-appearing brain tissue.

Table 2: Summary of SNR and CNR values in 5 healthy volunteers and 7 patients with MS

Imaging Technique	SNR	CNR (WM and GM)	CNR (WM and WM Lesions) (48 Lesions in 7 Patients)
FLAIR	19.3 ± 2.0	3.1 ± 0.7	7.1 ± 2.0
T2	23.9 ± 7.1	7.0 ± 3.0	13.9 ± 4.2
FLAIR^2	15.2 ± 2.3	7.1 ± 1.6	18.2 ± 6.1
DIR	4.5 ± 0.7	6.7 ± 1.1	9.4 ± 2.6

mutual information as a cost function. SNR and CNR were computed for FLAIR^2, FLAIR, and T2 in 5 healthy volunteers and 7 of our 9 patients with MS. Additionally, SNR and CNR for DIR were assessed for all patients with MS. The image noise was estimated within a large WM region as the SD of the subtraction of the consecutively acquired and coregistered images. The signal (S) was calculated as the mean signal within the same region in 1 of the 2 images, and SNR was calculated as SNR = $\sqrt{2}$ S / SD.[22] GM-WM CNR was computed as the signal difference between a representative part of the cortical GM and adjacent WM across multiple sections divided by the SD in the ROI of the subtraction image. In patients with MS, CNR was computed for up to 7 focal MS lesions and the surrounding WM within each patient.

RESULTS

Multiplication of the coregistered FLAIR with the T2-weighted scan results in an image (FLAIR^2) in which the CSF is suppressed due to the signal inversion on FLAIR and where WM signal is reduced due to the T2-weighted image contrast. Areas that are bright in both images, such as lesions and GM, are further enhanced in the resulting image. Figure 1 shows 3D-T2 (*A*), 3D-FLAIR (*B*), 3D-FLAIR^2 (*C*), and 3D-DIR (*D*) of a person with relapsing-remitting MS. Here, FLAIR^2 was acquired at 0.67 × 0.76 × 1.34 mm^3 and reconstructed to 0.3 mm^3 voxels, while DIR was acquired and reconstructed to 1 mm^3. Data acquisition took 6 minutes and 8 seconds for T2 and 7 minutes and 51 seconds for FLAIR, whereas the acquisition of DIR alone took 13 minutes and 35 seconds. The DIR shows some cortical areas of hyperintense signal, which appear normal on FLAIR^2.

SNR and CNR values are shown in Table 2. In summary, T2-weighted images had the highest SNR levels, while CNR levels were similar among 3D-DIR, 3D-T2, and 3D-FLAIR^2. Being the result of multiplication, FLAIR^2 had lower SNR than both FLAIR and T2. However, the CNR between GM and WM of FLAIR^2 was 133% higher than in FLAIR, and across the 48 analyzed lesions and their adjacent WM, FLAIR^2 achieved an improvement in CNR of 31%, 93%, and 158% compared with T2, DIR, and FLAIR, respectively.

An example of a high-spatial-resolution FLAIR^2 image of a patient with MS with cortical involvement is shown in Fig 2. A leukocortical U-fiber lesion is seen on sagittal FLAIR (*A*), FLAIR^2 (*B*), DIR (*C*), and T1-weighted (*D*) images, respectively. Here, FLAIR and T2 were acquired at 0.67 × 0.76 × 1.34 mm^3 and reconstructed to 0.3 mm^3 isotropic voxels. Additional coronal sections of the same lesion are shown (Fig 2). The T1-weighted image, which was acquired within 4 minutes and 12 seconds at the same spatial resolution, shows the lesion as a hypointense area.

The appearance of a large mixed GM-WM lesion on T2 (*A*), FLAIR (*B*), and FLAIR^2 (*C*) is compared in Fig 3. Here, FLAIR and T2 were acquired as described for the retrospective patient study. T2 exhibits the most signal within the lesion area and, in comparison with FLAIR, highlights how the WM lesion extends into the cortex. However, the heterogeneity of the lesion that is apparent on FLAIR is not seen on T2. FLAIR^2 can display a combination of these effects.

The large FOV of the sagittal 3D acquisition allows good visualization of lesions in the corpus callosum, infratentorial areas, and the cervical spine. In Fig 4, FLAIR^2 was calculated on the basis of the retrospectively analyzed patient study protocol. On axial (*A*), coronal (*B*), and sagittal (*C*) sections, an infratentorial, pontine lesion (*A* and *C*) and a corpus callosum (*C*) and a cervical spinal cord lesion (*B* and *C*) are visible.

Visually, the FLAIR^2 images reflected the quantitative assess-

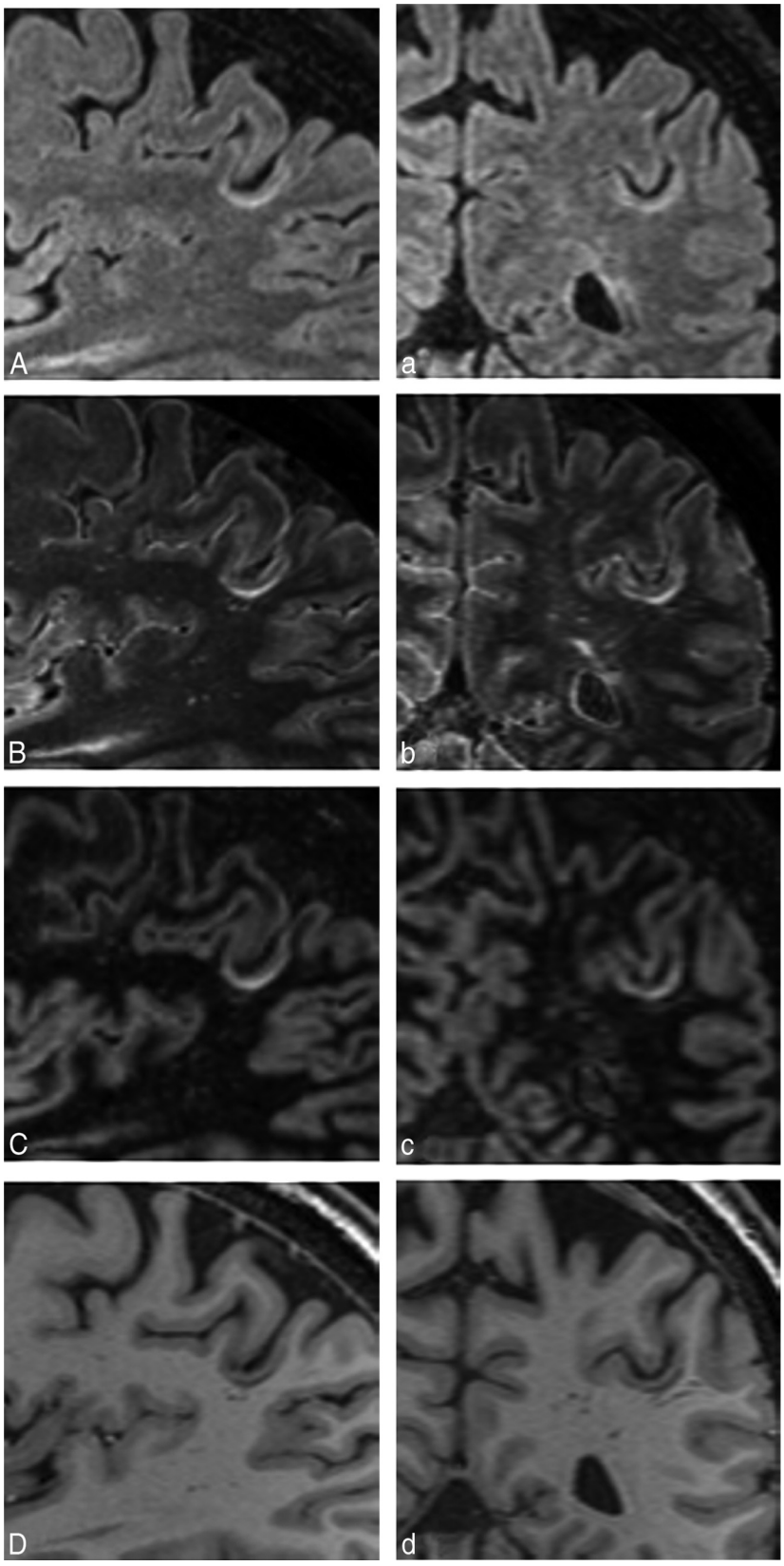

FIG 2. Depiction of a leukocortical U-fiber lesion on sagittal FLAIR (*A*), FLAIR^2 (*B*), DIR (*C*), and a T1-weighted image (*D*) of a patient with relapsing-remitting MS (a 54-year-old man). The same lesion is clearly visible on all coronal images (*a–d*). Here, FLAIR and T2 were reconstructed to 0.3-mm^3 isotropic imaging voxels (acquired at 0.6 × 0.68 × 1.2 mm^3 in 7 minutes and 51 seconds and 7 minutes and 12 seconds, respectively), resulting in a visible SNR reduction, especially on FLAIR (*A*), and influencing the image quality of our FLAIR^2 (*B*).

ment of CNR and SNR, showing excellent CNR between lesions and GM and WM. The conspicuity of cortical involvement was good, without false-positive areas often seen on DIR (On-line Figs 1 and 2). Scans with approximately 0.3-mm^3 voxel volume appear best for image quality and data-acquisition time.

DISCUSSION

Reliable detection of existing and new MS lesions is essential for the diagnosis and disease monitoring of MS. We presented a simple and robust approach for obtaining fluid-attenuated images with high contrast between lesions, GM and WM. Areas that are bright in both FLAIR and T2 are enhanced, whereas signal from areas that are dark in 1 of the 2 scans are suppressed. In particular, CSF remains hypointense on FLAIR^2. Moreover, because WM is more hypointense on T2-weighted images than on FLAIR and MS lesions are bright on both images, the FLAIR^2 images resemble DIR scans, but at much higher SNR and CNR compared with DIR (Fig 1 and Table 2). It may seem counterintuitive to multiply 2 images because the SNR of the resulting image will always be smaller than the SNR of any of the 2 input images. However, the CNR for both lesions-WM and GM-WM was larger in FLAIR^2 than in FLAIR, facilitating easier manual lesion detection and potentially better automated lesion segmentation.

Considerations for Data Acquisition

We acquired all scans in a sagittal orientation by using 3D sequences, allowing coverage of the whole brain and parts of the spinal cord with 1 scan. We tested a range of spatial resolutions and found that the SNR penalty at an imaging voxel size of 0.2 mm^3 appears to be too large (results are not shown here), while FLAIR^2 images with 0.3-mm^3 voxels (Figs 1 and 2) present excellent contrast and good SNR. The retrospective FLAIR^2 study acquired 3D-FLAIR within 5:04 minutes, 3D-T2 in 4:42 minutes, and 3D-DIR in 9:44 minutes. When these images were acquired with a resolution of 1 × 1.15 × 1 mm^3, acquisition times for 3D-T2 and 3D-FLAIR extended to 5:27 min-

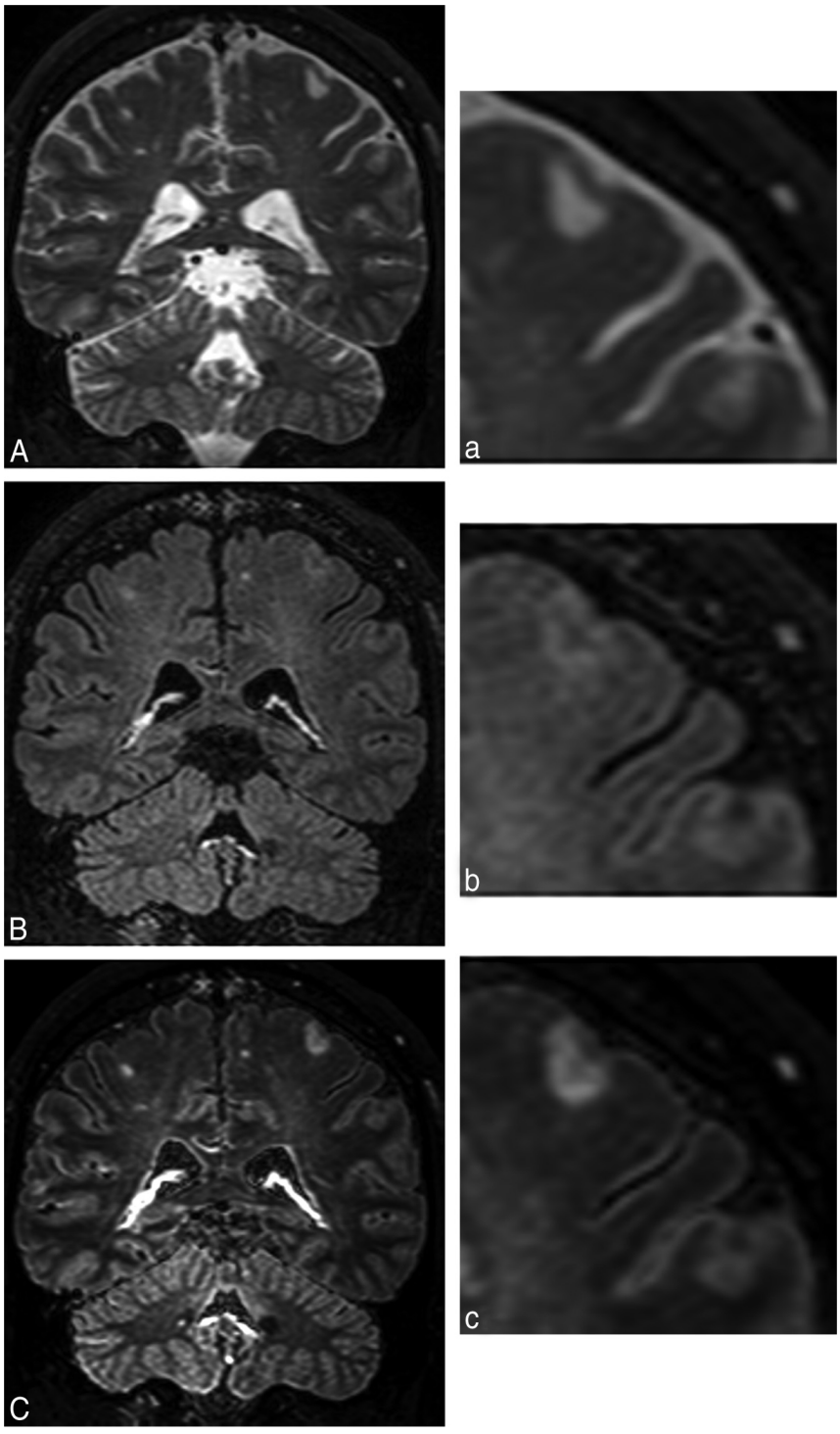

FIG 3. A large mixed GM-WM (leukocortical) lesion is present on T2 (*A*), FLAIR (*B*), and FLAIR^2 (*C*), acquired following the clinical imaging protocol in a patient with primary-progressive MS (a 44-year-old man). Their respective zoom-ins highlight the heterogeneity of the lesion, which is seen on FLAIR. Through the multiplication with T2, however, the lesion and its heterogeneity become more prominent (voxel size = 1.0 × 1.0 × 1.6 mm^3 acquired, 0.8 × 0.8 × 0.8 mm^3 reconstructed; T2 and FLAIR were acquired in 4 minutes and 43 seconds and 5 minutes, respectively).

utes and 6:56 minutes compared with 13:36 minutes for the 3D-DIR with the same spatial resolution. The gain in time and CNR by omitting DIR can be used to acquire the T2 and FLAIR scans at a higher spatial resolution.

The GM signal intensity on DIR scans varies considerably across the cortex, which is due to partial volume effects, variations in cortical thickness, and differences in relaxation times. The higher spatial resolution achievable with FLAIR^2 mitigates partial volume effects.

While FLAIR^2 could, in principle, be computed from 2D scans, performing sagittal 3D data acquisition has several advantages. The sagittal readout offers the possibility of using partial parallel imaging[23] along both phase-encoding directions. Subtle ghosting due to partial parallel imaging can be exacerbated on multiplication if the 2 images have similar ghosting characteristics. The use of different acceleration factors for FLAIR (eg, 2.5, 2) and T2 (eg, 2, 1.5) may help mitigate this effect. However, we did not test whether identical sensitivity encoding factors lead to any amplification of ghosting artifacts. The sagittal acquisition furthermore allows large FOVs along the foot-head direction that extend into the cervical spine, even with a conventional head coil (Fig 4). With dedicated head-neck coils, the brain, the cervical spine, and superior aspects of the thoracic spine can be imaged with 1 sagittal acquisition, which would capture most of the clinically relevant spinal cord lesions.[24]

Images acquired in 3D usually have isotropic voxels and, by definition, no intersection gap. Image registration works well with such data, which is essential for the FLAIR^2 approach. Moreover, 3D scans can be easily reformatted without loss of image quality. Due to the nonselective inversion pulse, there are no artifacts due to the inflow of noninverted blood and CSF in 3D-FLAIR images. Therefore, the additional proton density–weighted scan,[5] which is necessary for detecting infratentorial lesions in 2D protocols, becomes obsolete with 3D protocols (Fig 4). However, it has been suggested that low T2-weighting of fast FLAIR acquisitions[4] and the different T2-characteristics of infratentorial lesions[25] may limit their visibility on FLAIR. The combination of 3D-FLAIR and 3D-T2 should overcome insufficient T2-weighting in regions of the posterior fossa.

A study of 11 patients with relapsing-remitting MS and 5 with secondary-progressive MS at 1.5T showed that most infratentorial lesions were detected with 3D-FLAIR and 3D-DIR.[19] Finally, due to the high isotropic spatial resolution of 3D-FLAIR^2, corpus

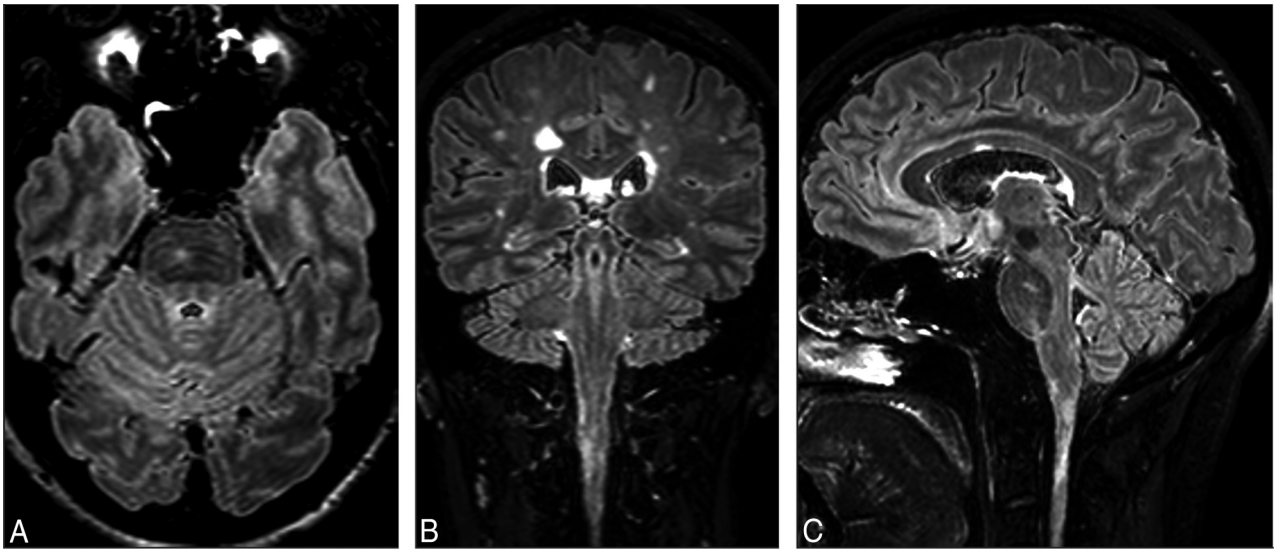

FIG 4. FLAIR^2 acquired at $1 \times 1 \times 1.6$ mm^3 and reconstructed to 0.51 mm^3 shows an infratentorial lesion located in the pons (*A* and *C*), a lesion in the cervical spinal cord (*B* and *C*), and a lesion in the corpus callosum (*C*) in the same patient with MS. Due to the isotropic spatial resolution, the large FOV, and the insensitivity to flow in the infratentorial parts of the brain, no additional 2D or proton-density weighted scans are required to visualize these lesions.

callosum lesions are detectable without a separate acquisition of a sagittal 2D-FLAIR (Fig 4). By omitting the acquisition of the sagittal 2D-FLAIR, the 2D proton density–weighted image, and potentially the DIR, approximately 20 minutes of acquisition time is saved, which can be invested in acquiring 3D sequences at higher spatial resolution, for instance. In research studies, the remaining scanning time can also be used in the acquisition of advanced MR images, such as myelin water,[26] magnetization transfer imaging,[27] or susceptibility-weighted imaging[28-30] for the calculation of frequency maps as measures of MS tissue damage[31] and of R2* maps.[32]

Improved Assessment of the Cortical GM

An improved visualization of the cortical GM and cortical damage is an important step in finding new markers for disease progression in patients with MS. Currently, GM thickness and GM lesion count are attractive markers. However, WM lesions close to GM or mixed GM-WM lesions are often misclassified. FLAIR^2 contrast could be helpful in automatically generating lesion masks. Automated segmentation should be improved, considering the high CNR between lesions and adjacent WM and surrounding GM.

Juxtacortical and leukocortical lesions are often seen within or close to the cortical U-fibers (Fig 2 and On-line Figs 1 and 2). It has been suggested that these areas promote lesion development due to reduced CSF circulation.[10] DIR suppresses the WM component of the signal, which aids in lesion classification. However, the SNR reduction and the detection of a considerable number of false-positive lesions aggravate the use of DIR to mirror cortical damage.

Limitations

The hyperintense rim on the surface of the brain seen on FLAIR is also visible on FLAIR^2. However, the rim becomes less prominent with increasing spatial resolution. The quality of FLAIR^2 depends on good image registration between the 2 input scans. Due to the brightness of the CSF signal in the T2-weighted scan, any misregistration would be immediately apparent on FLAIR^2. Here, we saw no signs of misregistration in >30 scans, suggesting that the approach can be implemented as a fully automated step on MR imaging systems. The robustness of image registration was previously demonstrated for the fusion of FLAIR and venograms computed from susceptibility-weighted images.[33,34] The resulting FLAIR* images feature lesions and veins, which are often associated with MS lesions, but less often with WM hyperintensities of different etiology. Image-registration artifacts are a particular caveat for the detection of subpial lesions because CSF signal may leak into the FLAIR^2 images, which could be falsely interpreted as lesions. However, separate evaluation of T2 and FLAIR in all 3 orthogonal imaging planes can mitigate this problem. Furthermore, FLAIR is known to present sometimes diffusely abnormal signal in the periventricular WM, even in healthy subjects. This effect of unknown origin is not reduced in FLAIR^2. Therefore, the definition of diffusely abnormal WM requires a scan that is not susceptible to this effect (eg, a proton density–weighted scan). Finally, the sensitivity and specificity of FLAIR^2 compared with FLAIR or DIR were not assessed in this proof-of-principle study.

CONCLUSIONS

The proposed approach results in fluid-attenuated images with improved CNR between lesions, WM and GM compared with conventional FLAIR scans. FLAIR^2 can be computed retrospectively from T2 and FLAIR, which are available in most clinical and research studies on MS. The wide availability of the input data and the simplicity of the technique allow other research groups to quickly verify the usefulness of FLAIR^2 in a wide range of settings. We propose a protocol of 3D-T1, 3D-T2, 3D-FLAIR, and FLAIR^2, which can be acquired within 20 minutes at a spatial resolution of 0.3 mm^3, compared with 33 minutes if DIR is included. This protocol captures WM lesions in the entire brain, including infratentorial regions, the corpus callosum, and most of the cervical cord (the entire cervical cord and parts of the thoracic cord if a head-

neck coil is used), and cortical lesions at high spatial resolution. With its DIR-like contrast, but higher SNR and CNR, FLAIR^2 may elegantly resolve the debate as to whether to include DIR in the standard imaging protocol of MS.

ACKNOWLEDGMENTS

The authors thank the participants of this study, Philips Healthcare for their continuing support, and the University of British Columbia MRI Research Centre and its staff and technologists for their support and service.

Disclosures: Vanessa Wiggermann—*UNRELATED*: *Travel/Accommodations/Meeting Expenses Unrelated to Activities Listed*: F. Hoffmann-La Roche, *Comments*: travel reimbursements; *OTHER RELATIONSHIPS*: recipient of a Doctoral Studentship Award from the MS Society of Canada (EGID 2002). Anthony Traboulsee—*UNRELATED: Board Membership*: F. Hoffmann-La Roche, *Comments*: Steering Committee member; *Consultancy:* Biogen, Teva, EMD Serono, Chugai, Roche, Genzyme, MedImmune; *Grants/Grants Pending*: Genzyme, F. Hoffman La Roche; *Payment for Lectures (including service on Speakers Bureaus)*: Genzyme, EMD Serono. David K.B. Li—*UNRELATED*: *Board Membership*: Opexa Therapeutics, Novartis, Nuron, and Roche, *Comments*: member of the Data and Safety Advisory Board for Opexa Therapeutics and the Scientific Advisory Board for Novartis, Nuron, and Roche; *Consultancy*: Vertex Pharmaceutical (advisor for product development); *Expert Testimony*: Genzyme,* F. Hoffmann-La Roche,* Merck-Serono,* Nuron,* Perceptives,* Sanofi-Aventis.* Alexander Rauscher—*RELATED*: *Grant*: Canadian Institutes of Health Research, *Comments*: Canadian Institutes of Health Research New Investigator Award (salary award); *UNRELATED*: *Board Membership*: F. Hoffmann-La Roche, *Comments*: Imaging Advisory Board. *Money paid to the institution.

REFERENCES

1. Stewart WA, Hall LD, Berry K, et al. **Correlation between NMR scan and brain slice data in multiple sclerosis.** *Lancet* 1984;2:412 Medline
2. Traboulsee A, Li DK. **Conventional MR imaging.** *Neuroimaging Clin N Am* 2008;18:651–73, x CrossRef Medline
3. Simon JH, Li D, Traboulsee A, et al. **Standardized MR imaging protocol for multiple sclerosis: Consortium of MS Centers consensus guidelines.** *AJNR Am J Neuroradiol* 2006;27:455–61 Medline
4. Okuda T, Korogi Y, Shigematsu Y, et al. **Brain lesions: when should fluid-attenuated inversion-recovery sequences be used in MR evaluation?** *Radiology* 1999;212:793–98 CrossRef Medline
5. Paty DW, Li DK, Oger JJ, et al. **Magnetic resonance imaging in the evaluation of clinical trials in multiple sclerosis.** *Ann Neurol* 1994; 36(suppl):S95–96 CrossRef Medline
6. Bermel RA, Fisher E, Cohen JA. **The use of MR imaging as an outcome measure in multiple sclerosis clinical trials.** *Neuroimaging Clin N Am* 2008;18:687–701, xi CrossRef Medline
7. Kutzelnigg A, Lucchinetti CF, Stadelmann C, et al. **Cortical demyelination and diffuse white matter injury in multiple sclerosis.** *Brain* 2005;128(pt 11):2705–12 CrossRef Medline
8. Lucchinetti CF, Popescu BF, Bunyan RF, et al. **Inflammatory cortical demyelination in early multiple sclerosis.** *N Engl J Med* 2011;365: 2188–97 CrossRef Medline
9. Calabrese M, Gallo P. **Magnetic resonance evidence of cortical onset of multiple sclerosis.** *Mult Scler* 2009;15:933–41 CrossRef Medline
10. Kutzelnigg A, Lassmann H. **Cortical demyelination in multiple sclerosis: a substrate for cognitive deficits?** *J Neurol Sci* 2006;245: 123–26 CrossRef Medline
11. Nielsen AS, Kinkel RP, Madigan N, et al. **Contribution of cortical lesion subtypes at 7T MRI to physical and cognitive performance in MS.** *Neurology* 2013;81:641–49 CrossRef Medline
12. Calabrese M, Poretto V, Favaretto A, et al. **Cortical lesion load associates with progression of disability in multiple sclerosis.** *Brain* 2012;135:2952–61 CrossRef Medline
13. Calabrese M, Romualdi C, Poretto V, et al. **The changing clinical course of multiple sclerosis: a matter of gray matter.** *Ann Neurol* 2013;74:76–83 CrossRef Medline
14. Redpath TW, Smith FW. **Technical note: use of a double inversion recovery pulse sequence to image selectively grey or white brain matter.** *Br J Radiol* 1994;67:1258–63 CrossRef Medline
15. Seewann A, Kooi EJ, Roosendaal SD, et al. **Postmortem verification of MS cortical lesion detection with 3D DIR.** *Neurology* 2012;78: 302–08 CrossRef Medline
16. Seewann A, Vrenken H, Kooi EJ, et al. **Imaging the tip of the iceberg: visualization of cortical lesions in multiple sclerosis.** *Mult Scler* 2011;17:1202–10 CrossRef Medline
17. Kilsdonk ID, de Graaf WL, Soriano AL, et al. **Multicontrast MR imaging at 7T in multiple sclerosis: highest lesion detection in cortical gray matter with 3D-FLAIR.** *AJNR Am J Neuroradiol* 2013;34:791–96 CrossRef Medline
18. Mugler JP 3rd, Bao S, Mulkern RV, et al. **Optimized single-slab three-dimensional spin-echo MR imaging of the brain.** *Radiology* 2000;216:891–99 CrossRef Medline
19. Moraal B, Roosendaal SD, Pouwels PJ, et al. **Multi-contrast, isotropic, single-slab 3D MR imaging in multiple sclerosis.** *Eur Radiol* 2008;18:2311–20 CrossRef Medline
20. Jenkinson M, Bannister P, Brady M, et al. **Improved optimization for the robust and accurate linear registration and motion correction of brain images.** *Neuroimage* 2002;17:825–41 CrossRef Medline
21. Jenkinson M, Smith S. **A global optimisation method for robust affine registration of brain images.** *Med Image Anal* 2001;5:143–56 CrossRef Medline
22. Price RR, Axel L, Morgan T, et al. **Quality assurance methods and phantoms for magnetic resonance imaging: report of AAPM nuclear magnetic resonance Task Group No. 1.** *Med Phys* 1990;17: 287–95 CrossRef Medline
23. Pruessmann KP, Weiger M, Scheidegger MB, et al. **SENSE: sensitivity encoding for fast MRI.** *Magn Reson Med* 1999;42:952–62 Medline
24. Okuda DT, Mowry EM, Cree BA, et al. **Asymptomatic spinal cord lesions predict disease progression in radiologically isolated syndrome.** *Neurology* 2011;76:686–92 CrossRef Medline
25. Bastianello S, Bozzao A, Paolillo A, et al. **Fast spin-echo and fast fluid-attenuated inversion-recovery versus conventional spin-echo sequences for MR quantification of multiple sclerosis lesions.** *AJNR Am J Neuroradiol* 1997;18:699–704 Medline
26. Prasloski T, Rauscher A, MacKay AL, et al. **Rapid whole cerebrum myelin water imaging using a 3D GRASE sequence.** *Neuroimage* 2012;63:533–39 CrossRef Medline
27. Loevner LA, Grossman RI, McGowan JC, et al. **Characterization of multiple sclerosis plaques with T1-weighted MR and quantitative magnetization transfer.** *AJNR Am J Neuroradiol* 1995;16:1473–79 Medline
28. Reichenbach JR, Venkatesan R, Schillinger DJ, et al. **Small vessels in the human brain: MR venography with deoxyhemoglobin as an intrinsic contrast agent.** *Radiology* 1997;204:272–77 CrossRef Medline
29. Haacke EM, Xu Y, Cheng YC, et al. **Susceptibility weighted imaging (SWI).** *Magn Reson Med* 2004;52:612–18 CrossRef Medline
30. Denk C, Rauscher A. **Susceptibility weighted imaging with multiple echoes.** *J Magn Reson Imaging* 2010;31:185–91 CrossRef Medline
31. Wiggermann V, Hernández Torres E, Vavasour IM, et al. **Magnetic resonance frequency shifts during acute MS lesion formation.** *Neurology* 2013;81:211–18 CrossRef Medline
32. Walsh AJ, Blevins G, Lebel RM, et al. **Longitudinal MR imaging of iron in multiple sclerosis: an imaging marker of disease.** *Radiology* 2014;270:186–96 CrossRef Medline
33. Grabner G, Dal-Bianco A, Schernthaner M, et al. **Analysis of multiple sclerosis lesions using a fusion of 3.0 T FLAIR and 7.0 T SWI phase: FLAIR SWI.** *J Magn Reson Imaging* 2011;33:543–49 CrossRef Medline
34. Sati P, George IC, Shea CD, et al. **FLAIR*: a combined MR contrast technique for visualizing white matter lesions and parenchymal veins.** *Radiology* 2012;265:926–32 CrossRef Medline